

Lithography-free positioned GaAs nanowire growth with focused ion beam implantation of Ga

Hermann DetzMartin Kriz, Suzanne Lancaster, Donald MacFarland, Markus Schinnerl, Tobias Zederbauer, Aaron Maxwell Andrews, Werner Schrenk, and Gottfried Strasser

Citation: *J. Vac. Sci. Technol. B* **35**, 011803 (2017); doi: 10.1116/1.4973340

View online: <http://dx.doi.org/10.1116/1.4973340>

View Table of Contents: <http://avs.scitation.org/toc/jvb/35/1>

Published by the [American Vacuum Society](#)

Articles you may be interested in

[Engineering carrier lifetimes in type-II In\(Ga\)Sb/InAs mid-IR emitters](#)

J. Vac. Sci. Technol. B **35**, 02B10102B101 (2016); 10.1116/1.4972978

[High resolution TEM analysis of focused ion beam amorphized regions in single crystal silicon—A complementary materials analysis of the teardrop method](#)

J. Vac. Sci. Technol. B **35**, 011801011801 (2016); 10.1116/1.4972050

Lithography-free positioned GaAs nanowire growth with focused ion beam implantation of Ga

Hermann Detz^{a)}

Austrian Academy of Sciences, Dr. Ignaz Seipel-Platz 2, 1010 Wien, Austria and Center for Micro- and Nanostructures and Institute for Solid-State Electronics, TU Wien, Floragasse 7, 1040 Wien, Austria

Martin Kriz, Suzanne Lancaster, Donald MacFarland, Markus Schinnerl, Tobias Zederbauer, Aaron Maxwell Andrews, Werner Schrenk, and Gottfried Strasser
Center for Micro- and Nanostructures and Institute for Solid-State Electronics, TU Wien, Floragasse 7, 1040 Wien, Austria

(Received 19 August 2016; accepted 13 December 2016; published 4 January 2017)

The authors report on a technique to grow GaAs nanowires at defined positions by molecular beam epitaxy without the need for a lithographic process. Here, a focused ion beam is used to implant Ga ions into Si (1 0 0) and Si (1 1 1) substrates, forming nanoscale droplets on the surface after an annealing step, which are in turn used as nucleation centers for self-catalyzed nanowire growth. This procedure completely avoids organic chemicals, as needed in other lithographic processes, and therefore allows nanowire growth in defined and flexible geometries, while being fully compatible with ultraclean environments. A minimum required pitch width is determined from implanted Ga point arrays, which were annealed to form droplets. The epitaxial yield for GaAs nanowires on Si (1 0 0) and Si (1 1 1) substrates is evaluated with respect to the acceleration voltage and implanted dose. The nanowire diameter is determined by thermodynamic properties at the growth surface while being insensitive to implantation parameters. © 2017 Author(s). All article content, except where otherwise noted, is licensed under a Creative Commons Attribution (CC BY) license (<http://creativecommons.org/licenses/by/4.0/>). [<http://dx.doi.org/10.1116/1.4973340>]

I. INTRODUCTION

Semiconductor nanowires have evolved from being considered a growth anomaly toward an established platform for heterogeneous material integration of III–V compound semiconductors with conventional Si-based electronics. Nanowire-based building blocks require defect- and contamination-free materials and positioned growth for the production of complex structures like light-emitting diodes, lasers, solar cells, or transistors.^{1–6} Au is preferred over other metals as the catalyst for vapor–liquid–solid (VLS) nanowire growth due to its low eutectic point with Si, Ge, or Ga.^{7,8} Despite its common use, the introduction of Au into semiconductor fabrication processes is problematic, as it forms deep trap states. Traces of the catalyst were, in particular, also identified along the sidewalls of VLS-grown nanowires.⁹

Alternatively, III–V nanowires can be grown in a self-catalyzed method by using the corresponding group III metal as the catalyst. Such processes were developed for the molecular beam epitaxy (MBE) of GaAs, $\text{In}_x\text{Ga}_{1-x}\text{As}$, and InAs to circumvent potential contamination with Au.^{10–12} Without position control, however, the nucleation process leads to a rather broad diameter distribution, as well as nanowire growth in random spots with local variations in their density.^{13,14}

Various lithographic processes for the positioning of catalyst metal have been developed. Yet, they all share the fact that they require organic substances as the etch mask, lift-off mask, imprint material, or simply as solvent.^{15,16} Epitaxial

growth on such templates, particularly in an ultrahigh vacuum environment, is only possible after extensive cleaning procedures. In order to avoid lithography steps, catalyst metals can be directly deposited through focused electron beam induced deposition, although organic precursors are still required in this case.¹⁷

We present a technique for position-controlled GaAs nanowire growth, which is initiated through focused-ion beam (FIB) deposition of catalyst droplets and therefore completely avoids the use of organic chemicals at any step. A similar approach was recently demonstrated for Si nanowires in a chemical vapor deposition growth process.¹⁸

II. EXPERIMENTAL PROCEDURE

This study was carried out on a set of Si (1 0 0) and Si (1 1 1) wafers from one ingot for each orientation. FIB implantation and MBE growth were done in parallel for one piece of each orientation. In a first step, Ga ions were implanted at defined sites by a FIB system. Point arrays were created through line scans using different dwell times but without beam blanking. This process was performed using acceleration voltages of 5, 15, and 30 kV, which effectively led to a variation in both the implantation depth and structural damage at the implantation sites. For each acceleration voltage, the implantation dose was varied over 1 order of magnitude within technical constraints, covering the range of 3.1×10^4 – 9.4×10^5 Ga⁺ ions per point, as outlined in Fig. 1. The projected mean implantation depth, which is also included in this plot, varies from 8.4 nm for 5 kV to 27.9 nm for a voltage of 30 kV.¹⁹

^{a)}Electronic mail: hermann.detz@tuwien.ac.at

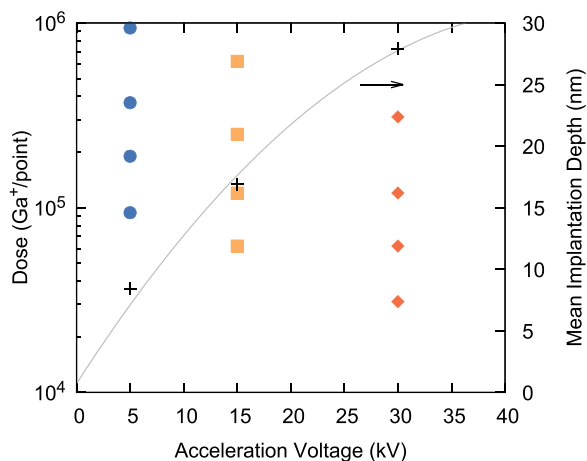


FIG. 1. (Color online) Overview of Ga⁺ dose vs acceleration voltage as used in this study. The dose was varied over 1 order of magnitude for each acceleration voltage, spanning the range of 3.1×10^4 – 3.1×10^5 Ga⁺/point for a voltage of 30 kV and 9.4×10^4 – 9.4×10^5 Ga⁺/point for a voltage of 5 kV, as shown by colored circles, squares, and diamonds. Black crosses indicate the projected implantation depth for the different acceleration voltages.

The substrates were then transferred into the MBE system. After initial outgassing steps in the loadlock system, they were brought to the desired nanowire growth temperature of 630 °C, measured with a pyrometer calibrated for GaAs, without intentional As₄ flux. For temperatures above 600 °C, the formation of Ga droplets with typical diameters around 80 nm could be observed, which is comparable to previously reported data.¹³ These droplets then served as nucleation centers for the nanowires, while the native oxide of the Si substrates, being stable up to 900 °C, reduces parasitic nanowire formation in between. GaAs nanowire growth was performed under Ga-rich growth conditions^{10,14} with typical equivalent layer Ga growth rates of 0.1 μm/h. Finally, the samples were cooled to room temperature under residual As₄ flux.

III. FIB-ASSISTED Ga-DROPLET NUCLEATION

The implantation of Ga ions by FIB allows the fabrication of ordered droplet arrays. An annealing step of 10 min at 600 °C leads to the formation of the Ga droplets, which can later be used as the nucleation centers for nanowire growth. Scanning electron microscope (SEM) images of samples corresponding to doses between 6.2×10^4 and 3.1×10^6 Ga⁺ per point at a constant voltage of 30 kV are shown in Fig. 2. Already the lowest dose shows regions of structural damage around the implantation spot. Increased doses lead to extended amorphized areas. Voids, caused by implantation doses above 3.1×10^6 Ga⁺/point, can lead to the formation of multiple droplets per point or to a lack of droplets with Ga-rich rim regions.

The solubility limit of Ga in Si is 4.5×10^{19} cm⁻³.²⁰ At the implantation spots, this limit is surpassed, leading to the formation of Ga droplets after annealing. Implanted doses between 6.2×10^4 and 3.1×10^6 Ga⁺ per point would lead to local concentrations of 1.1×10^{21} – 5.6×10^{22} Ga⁺/cm³, thus displacing most of the original Si host lattice.

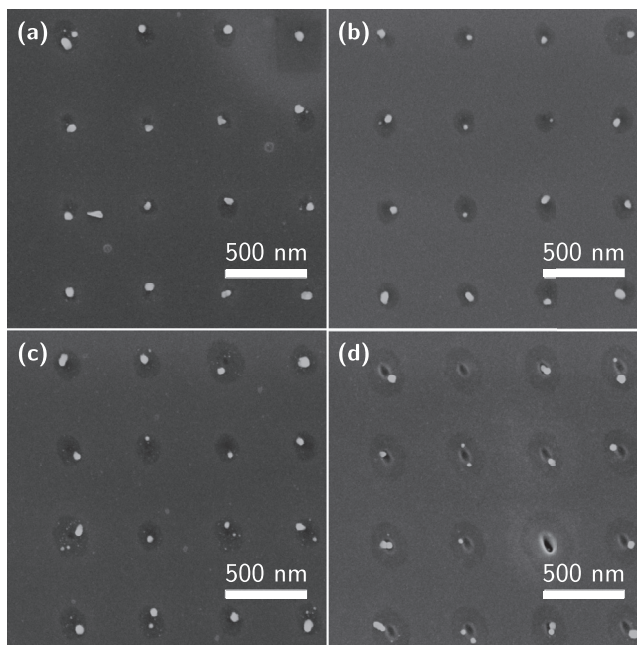


FIG. 2. Position controlled nucleation of Ga droplets on Si (100) surfaces for different FIB-implantation doses at a voltage of 30 kV: (a) 6.2×10^4 Ga⁺/point, (b) 1.2×10^5 Ga⁺/point, (c) 3.1×10^5 Ga⁺/point, and (d) 3.1×10^6 Ga⁺/point. The patterns were annealed for 10 min at 600 °C under vacuum conditions to facilitate the formation of the Ga droplets.

The dimensions of the damaged area around the implantation spots allow to gauge the minimum pitch required for the formation of individual droplets, which is 400–500 nm at 30 kV. This is corroborated in a series of implanted arrays using different spacings between 50 and 1000 nm. Corresponding SEM images for Si (1 0 0) substrates and pitch widths of 50 and 100 nm, shown in Figs. 3(a) and 3(b), exhibit aggregations of Ga rather than the formation of individual droplets, which prevent nanowire growth at defined positions and uniform diameters. Larger pitches of 200 and 400 nm in Figs. 3(c) and 3(d) lead to individual droplets, which become more uniform for larger point-to-point distances.

From the yield of droplet formation at the defined positions, a minimum required pitch for the growth of nanowire arrays can be determined. Obtained data for Si (1 0 0) and Si (1 1 1) substrates are summarized in Fig. 4. Both data sets show a similar trend with an onset of individual droplet formation between 100 and 200 nm, reaching yields well above 90% for a separation of 1000 nm. The yield on Si (1 1 1) appears around 20% higher as compared to (1 0 0) oriented substrates. To ensure well separated nucleation centers, the array pitch was increased to 1 μm for the nanowire growth studies, presented in Secs. IV and V.

IV. POSITIONED NANOWIRE GROWTH ON Si (1 0 0)

Nanoscale Ga droplets, as discussed in Sec. III, were investigated with respect to their suitability as nucleation centers for nanowires. Si (1 0 0) substrates with sets of Ga-implanted point arrays were used as templates for MBE grown GaAs nanowires. The yield of epitaxial nanowires, grown along the $\langle 111 \rangle$ directions of the Si substrate, which

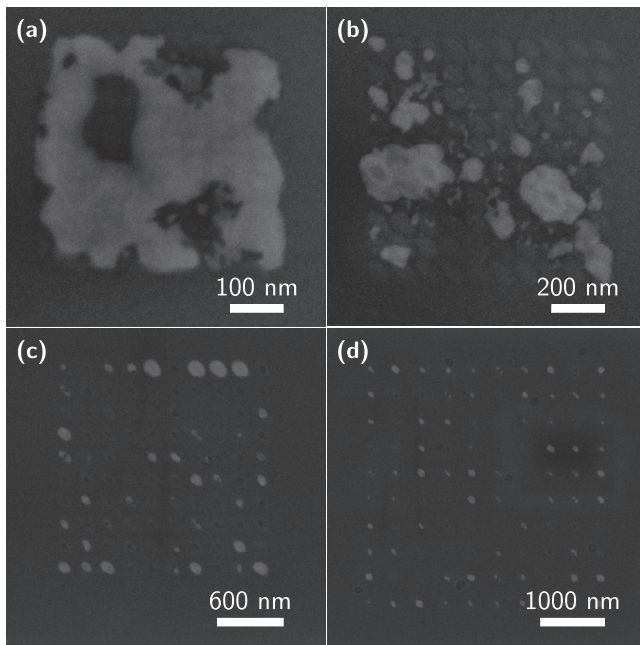


Fig. 3. Droplet arrays, implanted at 30 kV with a dose of 6.2×10^4 Ga⁺/point, with pitch widths of (a) 50 nm, (b) 100 nm, (c) 200 nm, and (d) 400 nm. The images were taken after a 10 min annealing step at 600 °C in vacuum. A pitch of 100 nm or less leads to aggregations of Ga, which are not suitable as a nanowire catalyst. Spacings of 400 nm and above lead to well defined uniform droplets.

thus grow under an angle of 54.7° to the substrate normal, at coordinates defined by the FIB implantation was chosen as a figure of merit. Nanowires, which do not originate from grid points or nanowires with different orientation, were excluded in this analysis. Statistical data were obtained from multiple arrays with 10 × 10 and 20 × 20 points.

The overview SEM images in Figs. 5(a)–5(d) show a clear dependence of the yield on the implanted dose as well as on the acceleration voltage. For the implantation voltage of 30 kV, lower doses lead to an increased nanowire yield, while for a voltage of 5 kV, the opposite behavior can be

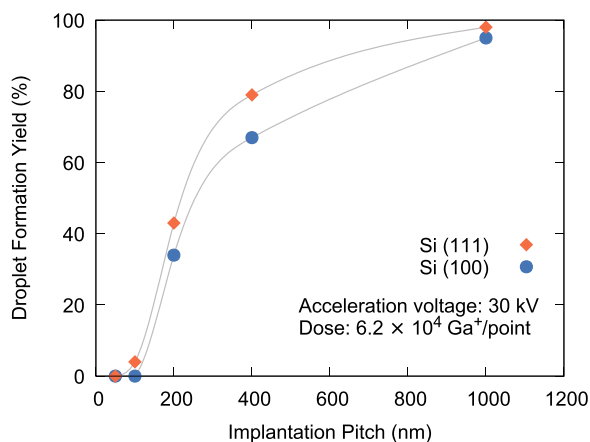


Fig. 4. (Color online) Yield of Ga droplet formation after FIB implantation and annealing at 600 °C under vacuum at a common dose of 6.2×10^4 Ga⁺/point. A minimum pitch of 200 nm is required for both, Si (1 0 0) and (1 1 1) substrates. Although the yield for Si (1 1 1) is slightly higher, both substrate orientations approach 100% for a pitch of 1000 nm.

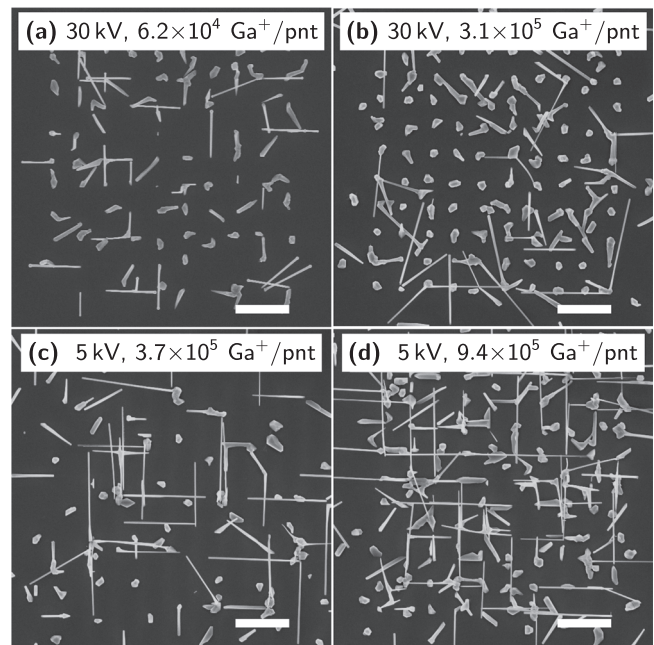


Fig. 5. GaAs nanowire arrays of 10 × 10 points, grown on a Si (1 0 0) substrate, where the nucleation sites were defined by FIB. (a) 30 kV, 6.2×10^4 Ga⁺/point, (b) 30 kV, 3.1×10^5 Ga⁺/point, (c) 5 kV, 3.7×10^5 Ga⁺/point, and (d) 5 kV, 9.4×10^5 Ga⁺/point. Scale bars are 2 μm wide.

observed. Parasitic growth within the array, particularly for implantation at 5 kV, can be attributed to a wider FIB beam area causing extended substrate damage and therefore additional nucleation spots.

The relation between implantation dose and nanowire yield for different acceleration voltages is plotted in Fig. 6. A clear trend toward higher yields for lower implantation doses can be observed for the 15 and 30 kV series. This behavior can be explained by the increasing structural damage for higher doses, which hinders epitaxial growth and causes deviations in the nanowire position. In contrast, the

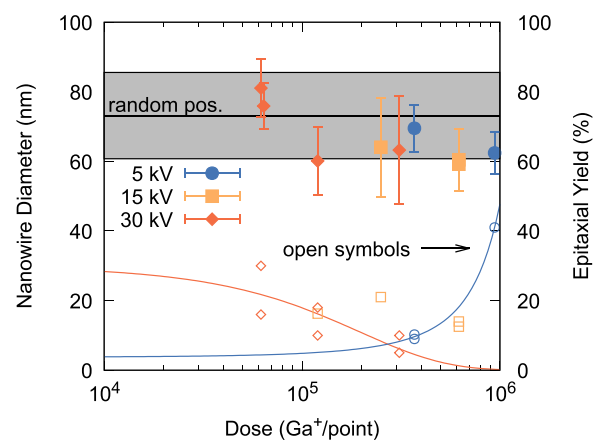


Fig. 6. (Color online) Yield of positioned epitaxial GaAs nanowires on Si (1 0 0) and corresponding diameters for several implantation doses and voltages. In the case of high acceleration voltages (15 and 30 kV), the yield is decreasing with the implanted dose. A low voltage of 5 kV shows the opposite behavior. Lines connecting the open data points serve as guides for the eye. The diameter and standard deviation for unpositioned nanowires, grown in the vicinity of the arrays, are sketched as a horizontal black line and gray shaded area.

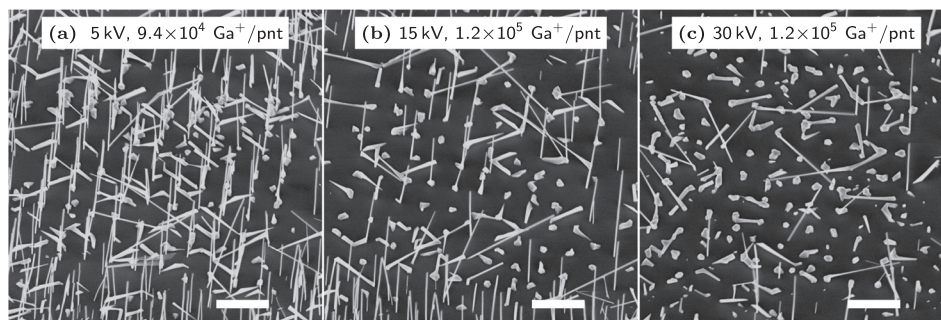


FIG. 7. FIB-positioned GaAs nanowire arrays, grown on a Si (1 1 1) substrate with a comparable implantation dose: (a) 5 kV, 9.4×10^4 Ga⁺/pnt, (b) 15 kV, 1.2×10^5 Ga⁺/pnt, and (c) 30 kV, 1.2×10^5 Ga⁺/pnt. Scale bars are 2 μ m wide. Lower acceleration voltage clearly leads to a higher yield of vertical nanowires at the predefined positions.

data points for 5 kV show a higher yield for a higher dose, which suggests that the structural damage can be neglected in that case.

Figure 6 also includes measured nanowire diameters for the different parameter combinations, which are also compared to the dimensions of nanowires grown at random positions in the vicinity of implanted arrays. In general, the measured range of nanowire diameters agrees well with data for Ga droplets of similar densities, nucleated at 630 °C on Si (1 0 0) surfaces with native oxide.¹³ Although lower doses seem to lead to slightly larger diameters around 78 nm, compared to 61 nm for higher implantation doses or 73 nm for random wires, this trend can be traced back to the nanowire density per unit area. More nanowires locally lead to a reduction of the III/V ratio and therefore to larger nanowire diameters.¹⁴

V. POSITIONED GROWTH ON Si (1 1 1)

A similar study, as described in Sec. IV, was performed on Si (1 1 1) substrates to investigate the positioned growth of vertical GaAs nanowires. SEM images for different acceleration voltages are presented in Figs. 7(a)–7(c). The individual arrays were chosen to have comparable doses. Due to the self-catalyzed nature of the growth process, parasitic nanowire growth outside the patterned area can not fully be excluded. Although an increased oxide thickness would reduce the number of randomly grown nanowires, they served as a reference for nanowire diameters under identical growth conditions in this case. The band surrounding the arrays, devoid of nanowires, allows to estimate a Ga surface diffusion length of 500 nm under growth conditions. This also imposes an upper limit for the pitch, as larger spacings would allow the spontaneous self-catalyzed nucleation of nanowires in between.

The lowest implantation voltage clearly leads to the highest yield of vertical nanowires within this series. A more detailed analysis is compiled in Fig. 8. The curves for high acceleration voltages (30 and 15 kV) again show opposite behavior compared to datapoints for 5 kV, similar as discussed in Sec. IV. While for large voltages the yield decays with increasing dose, implanted arrays at 5 kV reach the best yield for the highest dose (9.4×10^5 Ga⁺/point). In this case, the yield even surpasses 100%, which is caused by multiple

nanowires nucleating from the same implanted spot. This effect can be observed for doses above 1.9×10^5 at 5 kV due to the fact that the implanted spots are significantly larger compared to higher voltages.

Mean nanowire diameters, as extracted from SEM images, were found to vary between 48 and 57 nm for samples grown on Si (1 1 1) substrates, as plotted in Fig. 9. These values are slightly larger than 46.6 nm, which were measured for randomly nucleated nanowires in the vicinity of the implanted arrays. This deviation is attributed to the higher density of nanowires at random positions in the surrounding, which leads to a reduction of the III/V ratio, when compared to nanowires within the array.¹⁴ The mean diameter appears furthermore reduced by approximately 20%, when put into relation with positioned nanowires on Si (1 0 0) substrates.

VI. SUMMARY

Focused-ion beam assisted deposition is shown to be a viable alternative to established lithographic methods to achieve positioned GaAs nanowire growth on Si (1 0 0) and

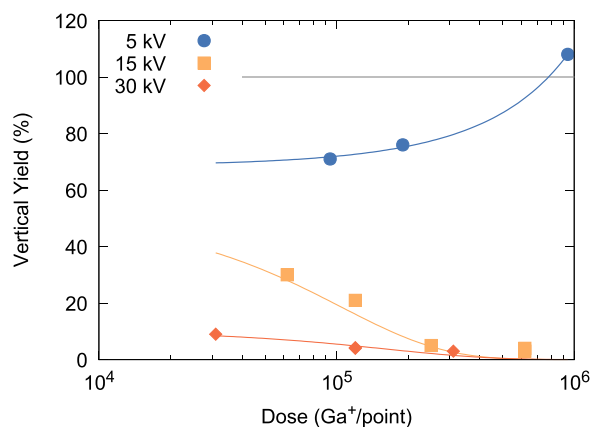


FIG. 8. (Color online) Yield of position-controlled vertical nanowires on Si (1 1 1) substrates with respect to acceleration voltage and implantation dose. Lower voltages commonly lead to a higher yield. While for the higher voltage series (30 and 15 kV), the yield decreases with increasing dose, the lowest voltage series shows the opposite behavior. For a dose of 8.4×10^5 and a voltage of 5 kV, the yield even surpasses unity. The nucleation of multiple nanowires per site can be observed due to the extended implantation area for doses larger than 1.9×10^5 Ga⁺/point at 5 kV. Data points are connected by lines, which serve as guide for the eye.

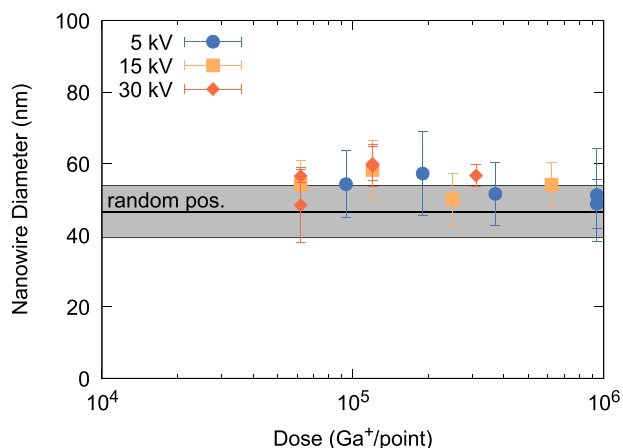


FIG. 9. (Color online) Nanowire diameter for different implantation doses and voltages on Si (1 1 1) substrates. The diameter and standard deviation of random nanowires in the vicinity of the arrays are plotted as a black horizontal line and gray shaded area for comparison. The diameters of positioned wires were found to be slightly larger (48–57 nm) compared to random nanowires (46.6 nm), which can be correlated with the lower nanowire density and therefore increased III/V ratio within the arrays.

Si (1 1 1) surfaces. Implanted Ga atoms form nanoscale droplets, after annealing at 600 °C or above, which can then be used as nucleation centers for VLS nanowire growth. Organic chemicals can be completely avoided, which renders this process fully compatible with ultrahigh vacuum environments.

Nucleation on implanted Ga point arrays at different pitches indicates a minimum spacing of 400 nm to ensure uniform individual catalyst droplets. Independent of the substrate orientation, higher acceleration voltages of 15 and 30 kV lead to a decreasing yield with higher implantation doses, which can be explained by structural damage to the host crystal around the defined coordinates. In contrast, larger doses at a relatively low acceleration voltage of 5 kV are shown to be more efficient for nanowire nucleation, approaching 40% on Si (1 0 0) substrates and above 100% on Si (1 1 1). Partially, this high yield is also caused by the nucleation of multiple nanowires per grid point due to larger implanted area, as compared to higher acceleration voltages. A better control of the implantation process parameters, particularly the dwell time and beam blanking, should allow increased yield as well as diameter uniformity.

Catalyst droplets formed by the implanted Ga initially provide preferential nucleation spots, yet the final morphology of the droplet is determined through the growth conditions like III/V ratio and substrate temperature.^{14,21,22} Consequently, the

nanowire diameter is found to be widely insensitive to the parameters of the implantation process. Minor deviations in the diameter with respect to nanowires at random positions can mainly be explained by a local variation of the nanowire density and therefore the III/V ratio.

ACKNOWLEDGMENTS

H.D. is a recipient of an APART Fellowship of the Austrian Academy of Sciences. The authors acknowledge financial support by the Austrian Science Fund (FWF): P26100-N27 (H2N), as well as through the “Gesellschaft für Mikro- und Nanoelektronik” GMe.

- ¹H. J. Fan, P. Werner, and M. Zacharias, *Small* **2**, 700 (2006).
- ²T. Bryllert, L.-E. Wernersson, T. Löwgren, and L. Samuelson, *Nanotechnology* **17**, S227 (2006).
- ³Y. Zhang, J. Wu, M. Aagesen, and H. Liu, *J. Phys. D: Appl. Phys.* **48**, 463001 (2015).
- ⁴A. M. Ionescu and H. Riel, *Nature* **479**, 329 (2011).
- ⁵Q. Gao *et al.*, *Nano Lett.* **14**, 5206 (2014).
- ⁶H. Sun, F. Ren, K. W. Ng, T.-T. D. Tran, K. Li, and C. J. Chang-Hasnain, *ACS Nano* **8**, 6833 (2014).
- ⁷P. Nguyen, H. T. Ng, and M. Meyyappan, *Adv. Mater.* **17**, 1773 (2005).
- ⁸T. Baron, M. Gordon, F. Dhalluin, C. TERNON, P. Ferret, and P. Gentile, *Appl. Phys. Lett.* **89**, 233111 (2006).
- ⁹J. B. Hannon, S. Kodambaka, F. M. Ross, and R. M. Tromp, *Nature* **440**, 69 (2006).
- ¹⁰A. Fontcuberta i Morral, C. Colombo, G. Abstreiter, J. Arbiol, and J. R. Morante, *Appl. Phys. Lett.* **92**, 063112 (2008).
- ¹¹M. HeiB, A. Gustafsson, S. Conesa-Boj, F. Peiró, J. R. Morante, G. Abstreiter, J. Arbiol, L. Samuelson, and A. Fontcuberta i Morral, *Nanotechnology* **20**, 075603 (2009).
- ¹²U. P. Gomes, D. Ercolani, V. Zanniri, J. David, M. Gemmi, F. Beltram, and L. Sorba, *Nanotechnology* **27**, 255601 (2016).
- ¹³H. Detz, M. Kriz, D. MacFarland, S. Lancaster, T. Zederbauer, M. Capriotti, A. M. Andrews, W. Schrenk, and G. Strasser, *Nanotechnology* **26**, 315601 (2015).
- ¹⁴F. Bastiman, H. Küpers, C. Somaschini, and L. Geelhaar, *Nanotechnology* **27**, 095601 (2016).
- ¹⁵T. Mårtensson, P. Carlberg, M. Borgström, L. Montelius, W. Seifert, and L. Samuelson, *Nano Lett.* **4**, 699 (2004).
- ¹⁶B. Bauer, A. Rudolph, M. Soda, A. Fontcuberta i Morral, J. Zweck, D. Schuh, and E. Reiger, *Nanotechnology* **21**, 435601 (2010).
- ¹⁷G. Hochleitner, M. Steinmair, A. Lugstein, P. Roediger, H. D. Wanzenboeck, and E. Bertagnolli, *Nanotechnology* **22**, 015302 (2011).
- ¹⁸M. Hetzel, A. Lugstein, C. Zeiner, T. Wójcik, P. Pongratz, and E. Bertagnolli, *Nanotechnology* **22**, 395601 (2011).
- ¹⁹J. F. Ziegler, M. D. Ziegler, and J. P. Biersack, *Nucl. Instrum. Methods Phys. Res., B* **268**, 1818 (2010).
- ²⁰C. W. White, S. R. Wilson, B. R. Appleton, and F. W. Young, Jr., *J. Appl. Phys.* **51**, 738 (1980).
- ²¹J. H. Paek, T. Nishiwaki, M. Yamaguchi, and N. Sawaki, *Phys. Status Solidi C* **6**, 1436 (2009).
- ²²T. Rieger, S. Heiderich, S. Lenk, M. I. Lepsa, and D. Grützmacher, *J. Cryst. Growth* **353**, 39 (2012).